ACS SENSORS

Article

Cite This: ACS Sens. 2017, 2, 1594-1601

pubs.acs.org/acssensors

Portable GMR Handheld Platform for the Detection of Influenza A Virus

Kai Wu,[†,⊥] Todd Klein,[†,⊥] Venkatramana D. Krishna,[‡,⊥] Diqing Su,[†,§] Andres M. Perez,[‡] and Jian-Ping Wang*[,†]

[†]Department of Electrical and Computer Engineering, University of Minnesota, Minneapolis, Minnesota 55455, United States

[‡]Department of Veterinary Population Medicine, College of Veterinary Medicine, University of Minnesota, St. Paul, Minnesota 55108, United States

[§]Department of Chemical Engineering and Material Science, University of Minnesota, Minneapolis, Minnesota 55455, United States

Supporting Information

ABSTRACT: Influenza A virus (IAV) is a common respiratory pathogen infecting many hosts including humans, pigs (swine influenza virus or SIV), and birds (avian influenza virus or AIV). Monitoring swine and avian influenza viruses in the wild, farms, and live poultry markets is of great significance for human and veterinary public health. A portable, sensitive, and quantitative immunoassay device will be of high demand especially in the rural and resource-limited areas. We report herein our Z-Lab point-of-care (POC) device for sensitive and specific detection of swine influenza viruses with minimum sample handling and laboratory skill requirements. In the present study, a portable and quantitative immunoassay platform based on giant magnetoresistive (GMR) technology is used for the detection of IAV nucleoprotein (NP) and purified H3N2v. Z-Lab displays quantitative results in less than 10 min with sensitivities down to 15 ng/mL and 125 $TCID_{50}$/mL for IAV nucleoprotein and purified H3N2v, respectively. This platform allows lab-testing to be performed outdoors and opens up the applications of immunoassays in nonclinical settings.

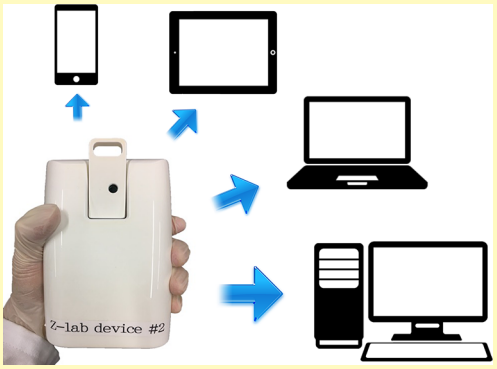

KEYWORDS: *Influenza A virus, point-of-care device, giant magnetoresistive, quantitative immunoassay platform, nonclinical*

Influenza A virus (IAV) is an enveloped negative sense RNA virus, which causes respiratory disease in many host species including humans, pigs and birds. A rapid and sensitive method for IAV detection is critical for controlling the infection and reducing the impact of possible influenza pandemic by early detection and intervention through medication or quarantine. Established laboratory methods for diagnosis of IAV include isolation of virus in embryonated chicken eggs or cell culture, immunological detection of viral antigens by lateral flow rapid influenza diagnostic tests (RIDTs), or enzyme linked immunosorbent assay (ELISA), serological detection of virus specific antibodies by ELISA, hemagglutination inhibition assay (HIA), or virus neutralization tests and detection of viral RNA by reverse transcription-polymerase chain reaction (RT-PCR).[1−4] Although virus isolation is sensitive method for diagnosis,[5] this technique is labor intensive and requires average of 3−7 days to obtain the results.[6] Immunological detection of viral antigens by RIDTs has low analytical sensitivity of 50−70% compared to virus isolation and PCR based methods. Although HIA and neutralization tests are widely used for diagnosis, antibodies are detected only after 8−14 days of onset of illness[7] and for proper diagnosis two serum samples with accurate timing are required. RT-PCR is highly sensitive and specific method; however, it involves an RNA extraction step and requires technical expertise as well as expensive laboratory instruments.[6,8]

Considerable efforts have been made to develop rapid, sensitive, and specific detection of IAVs using a nanotechnology approach. Among them, carbon nanotubes (CNTs), silicon nanowires (SiNW), quartz crystal microbalance (QCM), and gold nanoparticles are major platforms for ultrasensitive virus detection.[9−13] Those technologies use nanoparticles in combination with electrical or electrochemical detection and apply both nucleic-acid- and protein-based methods. A low cost ultrasensitive CNT electric immune assay was developed for detection of H1N1 swine influenza virus.[10] CNTs may enhance electrochemical reactivity of biomolecules, and this property was used for direct and label-free detection of IAV nucleic acids.[14] Recently, a highly sensitive electrical immunosensor to detect IAV H1N1 using single wall CNTs was developed.[15] Label-free and real-time detection of virus was also achieved through SiNW transistors and field effect transistors (FET).[16,17] SiNW sensor devices, when integrated with air sampling devices and microfluidic channels, was demonstrated to detect

Received: June 26, 2017
Accepted: October 17, 2017
Published: October 25, 2017

DOI: 10.1021/acssensors.7b00432
ACS Sens. 2017, 2, 1594−1601

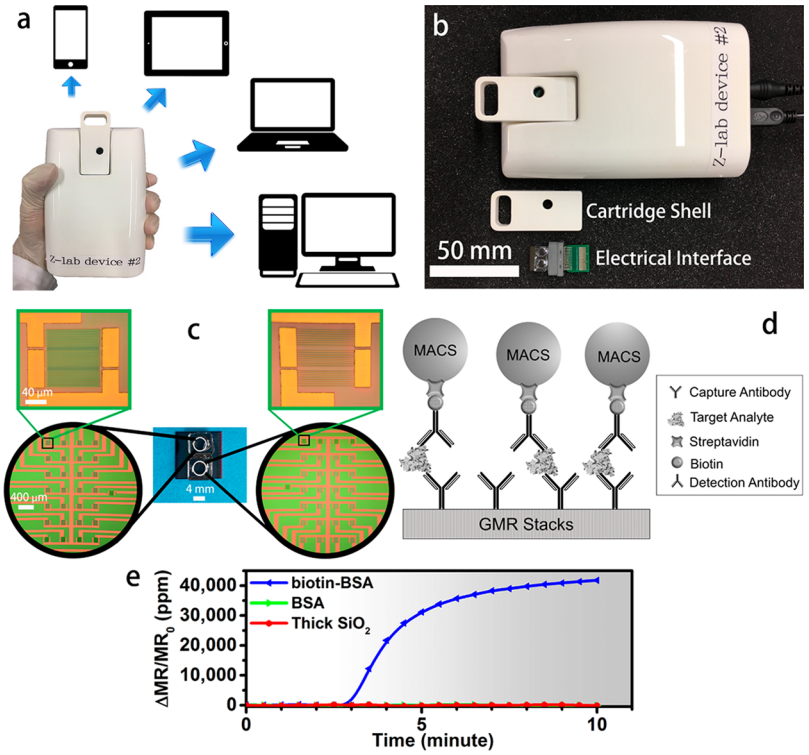

Figure 1. Z-Lab diagnosis platform and magnetic sandwich assay mechanism. (a) Real-time data collection and data transmission can be done either through wireless connection via Bluetooth to a smartphone, a tablet, and a laptop or through USB connection to a desktop computer. The established tablet/smartphone app and user interfaces can be found in Supporting Information S2. (b) The Z-Lab platform consists of three parts: a plastic cartridge, an electrical interface connecting the electrodes from GMR chip to the circuit board, and a handheld device. (c) Fabricated GMR chip. Each GMR chip consists of two independently working reaction wells which allows for two independent bioassays. Each reaction well consists of a 4 × 7 sensor array plus the 29th sensor on the 5th column. These 29 GMR sensors can be functionalized with different capture antibodies for multiplexed diagnostics. (d) A schematic view of magnetic sandwich assay. The high binding affinity between biotin and streptavidin-coated MACS allows a shorter assay time. Upon the capture of magnetic labels to the proximity of GMR sensors, the stray fields from magnetic labels changed local magnetization in the free layer thus changed the resistance and magnetoresistance of GMR sensors. (e) Real-time binding curves for targeted binding to positive control group (biotin-BSA coated sensors, blue curve), or nonspecific adhering to negative control group (BSA coated sensors, green curve). Sensor coated with a thick SiO_2 layer (5000 Å) serves as background signal (red curve).

airborne influenza virus.[18] A DNA aptamer based impedance biosensor for the specific detection of H5N1 avian influenza virus was also developed,[19] where DNA aptamers were used as an alternative to monoclonal antibodies. However, a portable diagnostic platform that is capable of performing on-site testing by nontechnicians instead of complicated laboratory tests by technicians is crucial in the field of animal disease surveillance and control. Recently, we have developed a simple and sensitive method for the detection of IAV based on handheld platform, giant magnetoresistive (GMR) biosensors and magnetic nanoparticles (MNPs) which complies with these aforementioned demands. GMR-based immunoassay technology has been successfully applied for the detection of different biomarkers and pathogens, such as mycotoxins,[20] aspergillus fumigatus allergen,[21] *Escherichia coli*,[22] chloramphenicol,[23] human interleukin 6 (IL-6),[24] and so forth. However, all of these immunoassays are limited to lab-based testing.

In this paper, we report a GMR handheld testing system, named as Z-Lab (see Figure 1a and b), and its usage in the detection of IAV. The basic approach of this detection system is similar to the ELISA approach to detect biomarkers: antibodies or antigens act as sensors which will capture a biomarker, then a detectable micro-object is added that will bind to the sensor-biomarker complex. The differences between our GMR handheld platform and ELISA is that GMR-based biosensing uses a GMR chip as its base and a magnetic label (or MNP) as its detectable nano-object. When the magnetic label binds to a sensor-biomarker complex, it detectably changes the resistance in the magnetic trilayer embedded in the chip (see Supporting Information S1). Because biological systems and samples are nonmagnetic, GMR-based biosensing has virtually no background noise to contend with.

Z-Lab has minimal operating requirements: a smartphone, tablet, or computer with a program that receives, interprets, and displays results as well as a wall adapter to charge the battery when needed. Z-Lab is about the size of a small digital multimeter, so it can easily be moved from place to place in a laboratory or point-of-care (POC) location. For personal use, it can perform tests at home, at work, or even on vacation. Z-Lab is fully integratable with modern mobile health platforms. It can wirelessly send data to a secure application on a smartphone, tablet, or computer, and that data can be securely transmitted, either with or without personal identifying data, to a cloud-based infrastructure which processes the data in light of standard dose−response curves. Real-time and past results are available via login.

EXPERIMENTAL SECTION

Virus Preparation. Influenza A virus strain A (H3N2) variant (H3N2v) was obtained from the University of Minnesota Veterinary Diagnostic Laboratory (St. Paul, MN). Virus was propagated in

DOI: 10.1021/acssensors.7b00432
ACS Sens. 2017, 2, 1594−1601

Madin-Darby canine kidney (MDCK) cells (ATCC CCL-34) in Dulbecco's modified Eagle's medium (DMEM) containing 0.5 μg/mL TPCK-trypsin (Worthington Biochemical Corporation, Lakewood, NJ) and purified from the clarified cell culture supernatants by ultracentrifugation through a 30% (w/v) sucrose cushion and stored in single use aliquots at −80 °C. Culture supernatant from uninfected MDCK cells were processed similarly to use for mock (control) preparation. The concentration of purified virus was determined by $TCID_{50}$ assay. For immunoassays, the virus was inactivated at 60 °C for 1 h. Both mock and virus preparation were treated with equal volume of lysis buffer containing 1% IGEPAL CA-630 (Sigma-Aldrich, product no. I8896) for 10 min at 37 °C to disrupt the virus particles. Different concentrations of virus were prepared by dilution in phosphate buffered saline (PBS) containing 3% BSA.

ELISA. IAV antigen capture ELISA was performed as described previously.[25] Briefly, 100 μL of 3 μg/mL anti-influenza A monoclonal antibody (MAB8800; EMD Millipore Corporation, Temecula, CA) specific for influenza A NP was coated in 96-well ELISA plates (Corning Inc., Corning, NY). After overnight incubation at 4 °C, the wells were blocked with 5% skim milk in PBS for 2 h at room temperature. Heat inactivated IAV H3N2v were diluted in sample diluent (3% BSA in PBS), and 100 μL of each sample was added to duplicate wells and incubated for 1 h at 37 °C. After washing the wells three times with wash buffer (0.05% tween 20 in PBS), 100 μL of 1 μg/mL biotinylated anti-influenza A monoclonal antibody (MAB8257B; EMD Millipore Corporation, Temecula, CA) was added and incubated for 1 h at room temperature. Wells were washed three times with wash buffer and incubated with 100 μL of 1:4000 diluted streptavidin-horseradish peroxidase (HRP) (Thermo scientific, Rockford, IL) for 30 min at room temperature. After washing the wells, 100 μL of TMB peroxidase substrate (Thermo scientific, Rockford, IL) was added and the reaction was stopped after 30 min incubation at room temperature by adding 100 μL of 1N H_2SO_4. The absorbance at 450 nm was measured by microtiter plate reader (Thermo Labsystems). The cut off value for distinguishing positive from negative was set as 0.20, which was calculated as mean of negative control absorbance values multiplied by 2.

GMR Nanosensor Array. The multilayer GMR film with top-down structure of Ta(50 Å)/NiFe(20 Å)/CoFe(10 Å)/Cu(33 Å)/CoFe(25 Å)/IrMn(80 Å)/Ta(25 Å)[25,26] was deposited onto 4 in. Si/SiO_2 wafers using a six-target Shamrock Magnetron Sputter System at the University of Minnesota. Each 4 in. GMR wafer yields 21 usable chips. Each chip contains two GMR sensor arrays that can be used for two independent immunoassays (see Figure 1c). Each GMR sensor array contains 29 sensors with 5 of them passivated with a very thick SiO_2 layer as negative control group (see Figure 1e), each GMR sensor can work independently, and in an ideal case this GMR sensor array is able to perform a multiplex detection of up to 24 biomarkers from one biological sample in one immunoassay. Each GMR sensor is connected to one peripheral bonding pad by the Cr(250 Å)/Au(2500 Å)/Cr(150 Å) lead. To protect the leads from scratch, a 5000 Å thick SiO_2 layer was deposited via electron beam evaporator, but excluding only the active sensors. Two passivation layers of Al_2O_3(180 Å)/SiO_2(150 Å) were deposited on the active sensors to prevent the corrosion from chemical reagents and biological samples as well as providing hydroxyl groups for sensor surface biofunctionalization. The Au layer in the bonding pad area is exposed by the etch back process using ion milling, which favors a better connection and signal transport with the external integrated circuits. All the chips were annealed at 200 °C for 1 h under 5 kOe magnetic field and then naturally cooled down to room temperature to align the magnetization of the pinning layer to the short axis. The magnetization of the free layer was set along the long axis due to shape anisotropy. This configuration of perpendicular alignment allowed the sensors to work at the most sensitive region of magnetoresistance transfer curves.

Each GMR chip is in the size of 16 mm × 16 mm with two independent sensor arrays symmetrically located on the opposite sides. Each sensor with size of 150 μm × 100 μm contains three GMR strip groups connected in series, and each group contains eight sensor strips connected in parallel. Each strip with the size of 150 μm × 750 nm is separated by a 4 μm spacer.

GMR Chip Surface Chemistry. Annealed GMR chips were triple washed with acetone, methanol, and isopropyl alcohol solutions and then blow dried. These chips were etched by oxygen plasma for 30 s and then placed under ultraviolet light and ozone (UVO) for 15 min to remove organic contaminants. Then each chip was soaked in 5 mL of 1% 3-aminopropyltriethoxysilane (APTES) in anhydrous toluene for 15 min to allow the covalent binding between APTES and hydroxyl groups from SiO_2 passivation layer.[27] The chips were then rinsed with acetone followed by ethanol and blow dried. A solution of 5% glutaraldehyde (Glu) in DI water was incubated on the sensor array areas for 5 h in order to bind aldehyde groups from Glu with amino groups from APTES. Aldehyde group from the other end of Glu allowed subsequent binding of capture antibodies onto GMR sensors.

Influenza A capture antibody (BE0159, Bio X Cell, West Lebanon, NH, USA, InVivoMab anti-Influenza A virus NP, clone H16-L10−4R5 (HB-65)) was robotically spotted over each sensor in 360 pL/droplet for three times (a total volume of ∼1 nL per sensor) by a programmable liquid dispensing system (sci-FLEXARRAYER S5, Scienion, Germany; Supporting Information S3). The control sensors were spotted with either bovine serum albumin (BSA) at 1 mg/mL or biotinylated bovine serum albumin (biotin-BSA) at 1 mg/mL in a similar fashion (Supporting Information S4). The prepared chips were incubated in a humidity chamber at 4 °C for 12 h to allow the immobilization of capture antibodies/BSA/biotin-BSA onto GMR sensor surface. Two bottomless wells made of poly(methyl methacrylate) (PMMA) were attached onto each chip centered at each sensor array area. Each well can hold a maximum volume of 50 μL of liquid. Subsequently, the sensor area was covered with 1 mg/mL BSA for 30 min to block other binding sites in order to avoid the nonspecific binding of subsequent biomolecules to GMR sensor surface, and then triple rinsed with PBST (0.05% Tween 20 in phosphate buffered saline) to thoroughly remove unbound BSA. 50 μL of recombinant influenza H1N1 nucleoprotein (IAV NP, Sino Biological Inc. Beijing, China) or purified H3N2v were added to each well and incubated for 1 h to allow the conjugation between target biomarkers and capture antibodies. After triple rinsing the sensor arrays with PBST, 50 μL of IAV detection antibody (MAB8257B, EMD Millipore Corporation, Temecula, CA, a mouse anti-influenza A monoclonal antibody specific for IAV NP) was added to each well and incubated for another 1 h to allow the conjugation between detection antibodies and target biomarkers. Finally, sensor arrays were triple rinsed with PBST before use.

Magnetic Labels. The magnetic labels were commercially available from Miltenyi Biotec, Inc. (2×10^{12} particles/mL; catalog no. 130-048-101, Auburn, CA), referred to as MACS. The MACS particles consist of small Fe_2O_3 nanoparticles embedded in a matrix of dextran.[28,29] The average overall hydrodynamic size of MACS particles is ∼60 nm measured by dynamic light scattering, and the average size of Fe_2O_3 nanoparticles is ∼8 nm measured by scanning electron microscopy (Supporting Information S5). Owing to the small size of Fe_2O_3 nanoparticles, the MACS particles are superparamagnetic which effectively helps avoid aggregation and precipitation of particles. Compared to other iron oxide nanoparticles, these MACS particles yield the highest magnetization under the applied field of 30 Oe,[30] which makes them the best candidates as magnetic labels for GMR-based immunoassays. The MACS particles were functionalized with streptavidin to yield high binding affinity with biotins from the end of IAV detection antibodies.

Z-Lab Signal Collection. Z-Lab monitors the real-time change of magnetoresistance ratio (ΔMR) from each GMR sensor. The initial magnetoresistance ratio (MR_0) of each sensor was calibrated at the first round of data collection. Because there were 29 sensors (5 control sensors covered with 5000 Å of SiO_2 and 24 active sensors coated with BSA, or biotin-BSA, or capture antibody−analyte−detection antibody sandwiches) from each sensor array, it took 1 s to collect and store an averaged MR from one biosensor. The MR data was collected sequentially, and it took 29 s to go through all the sensors. After a new measurement started, the real-time MR ratio of each sensor was

DOI: 10.1021/acssensors.7b00432
ACS Sens. 2017, 2, 1594−1601

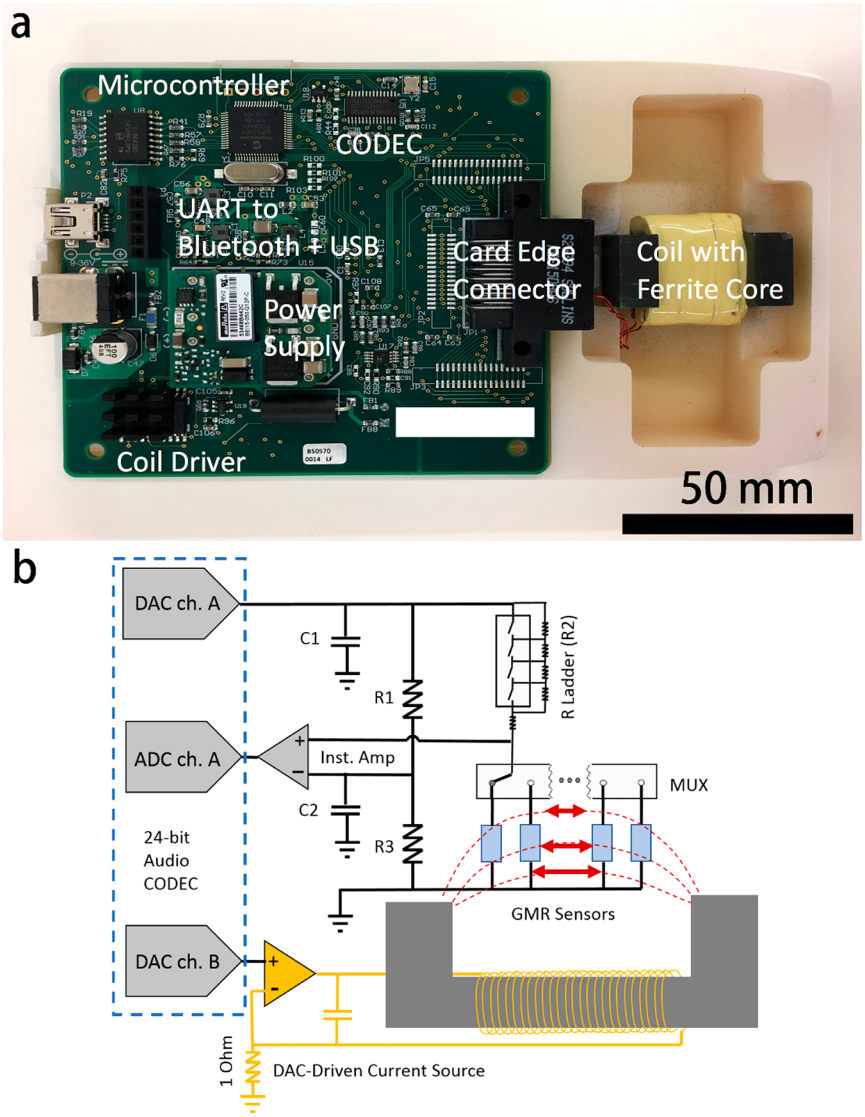

Figure 2. Z-Lab handheld device circuit board and circuit diagram. (a) Photograph of the circuit board inside Z-Lab handheld device. (b) Circuit diagram. The uniformity of magnetic field generated by coils are discussed in Supporting Information S6.

monitored for 3 min (each sensor was scanned 6 times), and then 50 μL of MACS solution was added into reaction well and ΔMR was monitored for another 7 min (each sensor was scanned for 14 times during this time span). A complete signal collection step only took 10 min.

SEM Collection. To further confirm the binding of magnetic labels to sensor surface, those GMR chips were investigated under scanning electron microscopy (SEM, JEOL 6500) at the Characterization Facility, University of Minnesota. After each measurement, the MACS solution was aspirated from the reaction well. Subsequently, the bottomless PMMA well was removed and the sensor array region was rinsed with DI water for 1 min to thoroughly remove the unbound magnetic labels and then blow dried. The GMR chips were coated with 50 Å of platinum (Pt) before investigation under SEM. As shown in Figure 3a, the area density of bounded magnetic labels increased with the concentration of analytes.

RESULTS AND DISCUSSION

Z-Lab Diagnosis Platform. The Z-Lab Diagnosis Platform provides highly sensitive and quantitative detection of biological molecules through the proper functionalization of magnetic labels and the 29 GMR sensors. Samples are loaded into the disposable cartridges and incubated within a reaction well surrounding the GMR sensors. The portable and low-cost construction leverages smartphone capabilities such as data processing, display, wireless communication (see Figure 1a), and GPS location services depending on the needs of each specific application.

Design of Circuit Board. The circuit board design consists of a microcontroller, 24-bit Audio CODEC, Wheatstone Bridge, current-source coil driver, and supporting hardware for both USB and Bluetooth communication (see Figure 2a). The purpose of the Wheatstone Bridge in this case is not to create perfect balance, but only to offset the bulk of the carrier tone frequency (f1) within the GMR voltage so that the bridge output voltage can be amplified at the instrumentation amplifier stage. The analog multiplexer and 30-pin chip adapter allows up to 29 GMR sensors, whose resistance are modulated by an external applied magnetic field (f2). Sensor-to-senor and/or chip-to-chip variation in resistance can be handled at system startup with the resistance ladder topology. Capacitors C1 and C2 are used to balance the parasitic capacitance found in both the multiplexer and the resistance ladder (see Figure 2b).

DOI: 10.1021/acssensors.7b00432
ACS Sens. 2017, 2, 1594−1601

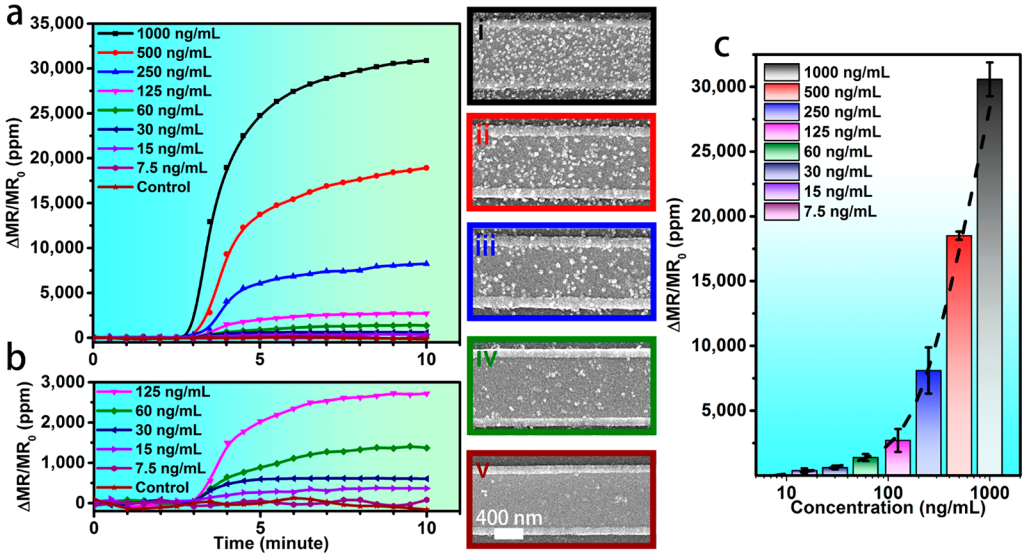

Figure 3. Real-time binding curves and averaged signal from different concentrations of IAV NP and negative control. (a) Binding curves in real-time for different concentrations of 50 μL of IAV NP samples measured by Z-Lab handheld device. In each measurement, the background signal was collected for 3 min, then 50 μL of MACS was added into reaction well and signal was collected for another 7 min. A small section of the GMR sensors was imaged with SEM (color-coded boxes represent the different concentrations of IAV NP, (i–v) in this figure) to compare the number of Magnetic labels bound to the sensors with that of $\Delta MR/MR_0$ signal. (b) Enlarged real-time binding curves from (a). (c) Averaged signals from different concentrations of 50 μL of IAV NP samples. The cutoff value for detecting IAV NP by our Z-Lab handheld system is 7.5 ng/mL. Error bars represent standard deviations of the signals from duplicate GMR sensors. The *y*-axis is presented as changes in MR normalized to initial MR in ppm (parts per million, Supporting Information S1).

In addition to the signal generation and collection, the circuit board also allows communication via both USB and Bluetooth. In the case of Bluetooth, we simply used the BlueSMiRF modem from SparkFun. This allows us to run the system on a smartphone and thereby dramatically increase the portable functionality for a very minor additional cost.

Z-Lab Signal Acquisition. The 24-bit audio CODEC generates sine waves to be driven across both the Wheatstone Bridge (f1) and the coil driver current source (f2). These signals combine through amplitude modulation via the GMR transfer function as described in previous literature.[26,29,31]

GMR Biosensor and Detection Principle. The Z-Lab uses a magnetic sandwich assay mechanism directly on top of the GMR biosensors (see Figure 1d). Excluding the control sensors which were either coated with BSA or biotin-BSA, the experimental sensors were coated with capture antibody–analyte–detection antibody sandwiches. The detection antibodies were labeled with biotin, which yielded high binding affinity to streptavidin. Once the streptavidin-coated magnetic labels (MACS, Miltenyi Biotec, Inc., Auburn, CA) were added into the reaction well, those magnetic labels were captured to the sensor surfaces due to Brownian motion and strong binding affinity between biotin and streptavidin. The magnetic labels, magnetized by the external in-plane magnetic field and GMR layer stray field,[32,33] became magnetic dipoles and generated stray fields that were detected by the GMR biosensors underneath the sandwich structure. A higher concentration of analytes resulted in a larger number of magnetic labels captured to the proximity of GMR sensor surface, thus the free layer in GMR biosensor experienced a larger dipole field from those magnetic labels, leading to an increased magnetic susceptibility in the free layer, thus, a positive signal from the sensor (Supporting Information S1). The free-floating magnetic labels that were not captured to the sensor surfaces would not contribute to the positive signal.[34,35] To eliminate the effect of nonspecific binding, the background signals from BSA-covered negative control sensors were subtracted from the positive signals from experimental sensors. The positive control sensors which were covered with biotin-BSA worked as a marker of the starting point of binding process (see Figure 1e).

Z-Lab Handheld Platform for Detection of IAV Nucleoprotein (NP). The real-time binding curves for IAV NP are shown in Figure 3a. The MR data was collected from each sensor for 3 min, and then 50 μL of MACS solution was added into reaction well and signals were collected for another 7 min. The MR increased immediately after the addition of magnetic labels. $\Delta MR/MR_0$ was introduced as an indicator of signal change due to the binding of magnetic labels to the proximity of sensor surface. As summarized in Figure 3b, the averaged signal from control group (mock) was 25 ppm, compared to 32 ppm for 7.5 ng/mL IAV NP and 368 ppm for 15 ng/mL IAV NP. The averaged signals from 30, 60, 125, 250, 500, and 1000 ng/mL IAV NP samples were 610, 1380, 2700, 8100, 18509, and 30 585 ppm, respectively. The cut off value for distinguishing positive from negative was set to be the twice as much signal as negative control which was 50 ppm. Therefore, our Z-Lab reached the limit of detection (LOD) for 50 μL of IAV NP sample at 15 ng/mL. In this experiment, our Z-Lab successfully distinguished between different concentrations of IAV NP samples within 10 min, a 50 μL sample with a higher concentration of IAV NP yielded a higher $\Delta MR/MR_0$, as expected.

ELISA for Detection of IAV NP. ELISA was carried out to compare the performance of Z-Lab. Our previous studies demonstrated that the antibodies used in this assay can detect multiple IAV strains.[25] When tested with purified H3N2v, the detection limit of ELISA was 250 $TCID_{50}$/mL (see Figure 4c).

Performance Comparison between Z-Lab and ELISA for the Detection of Purified H3N2v. Purified H3N2v samples were used to evaluate the performances of Z-Lab and

DOI: 10.1021/acssensors.7b00432
ACS Sens. 2017, 2, 1594–1601

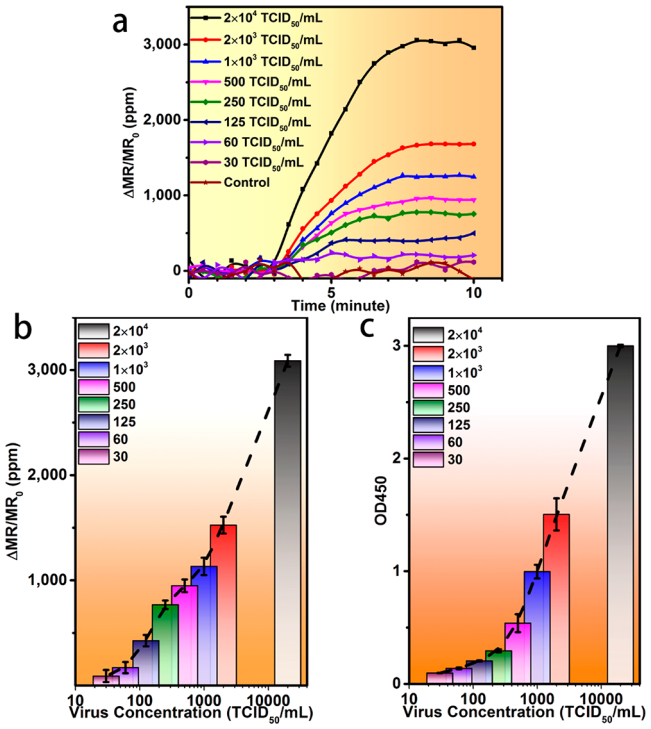

Figure 4. Real-time binding curves, averaged signal from different concentrations of purified H3N2v and negative control. Swine IAV strain H3N2v or control (mock) was treated with 1% IGEPAL CA-630 to disrupt virus particle and used for detection by GMR biosensor and ELISA. (a) Binding curves in real-time from Z-Lab handheld device. (b) Signals averaged from 50 μL of different concentrations of purified H3N2v samples using our Z-Lab handheld device. The LOD is 125 $TCID_{50}$/mL for Z-Lab. (c) Signals averaged from 100 μL of different concentrations of IAV purified H3N2v samples using ELISA technique. The LOD is 250 $TCID_{50}$/mL for ELISA.

ELISA. ELISA used 100 μL of biological sample, while our Z-Lab handheld platform used as little as 50 μL. The real-time binding curves from purified H3N2v were monitored with Z-Lab and are plotted in Figure 4a. Averaged magnetic signals are summarized in Figure 4b showing that the signal from negative control group was 89 ppm with a standard deviation of 36 ppm. While the signal from 30, 60, and 125 $TCID_{50}$/mL samples were 90, 171, and 427 ppm, respectively. Thus, the LOD for detecting 50 μL of purified H3N2v sample is 125 $TCID_{50}$/mL from our Z-Lab handheld platform. ELISA showed similar signal trend on purified H3N2v samples, with a LOD of 250 $TCID_{50}$/mL for 100 μL biological sample. Taking the sample volume into consideration, our Z-Lab yielded a higher detection limit than ELISA. The nasal samples of infected swine have been reported to contain 10^3–10^5 $TCID_{50}$/mL virus,[36] which is above the limit of detection of this assay.

Capabilities of GMR Sensors and the Performance of Z-Lab Handheld Platform. All the GMR sensors were fabricated at the Minnesota Nano Center, University of Minnesota. The initial MR ratio of each sensor under the applied field of −30 Oe to +30 Oe is around 2%, with around ±5% difference from sensor to senor on one chip, and there is ±10% differences from chip to chip. Which is one of the factors causing the error bars in Figures 3c and 4b. However, this difference caused by GMR sensors is acceptable considering the state-of-art nanofabrication technology. The main factor causing the deviations of collected signals from sensor to sensor (or chip to chip) lies in the handling of biological samples and biofunctionalized GMR chips. It is recommended that the completely biofunctionalized GMR chips should be stored under the conditions of 4 °C and 95% humidity, and should be used for testing within 1 week. However, those GMR chips functionalized with APTES and Glu can be stored under dry and dark conditions for several months without losing their reactivity.

CONCLUSIONS

In summary, we have successfully developed a portable diagnostic platform, Z-Lab, which is capable of performing on site testing of IAV in swine with minimum sample handling and laboratory skill requirements. Influenza virus, if present in the sample, will cause magnetic tags to bind to the GMR sensor through a sandwich structure, resulting in change in MR. This real-time electrical signal can be detected by our Z-Lab handheld device, which is capable of data processing, display, wireless communication, and GPS location services depending on the needs of specific application.

This Z-Lab system is the first version of a prototype that has been developed for point-of-care diagnostics. The GMR chips used in this system give its strong multiplex capability, which can significantly reduce costs associated with laboratory testing and enable widespread medical and environmental testing in homes, in the field, and at point-of-care clinics. The ultimate goal of our GMR-based handheld platform is to realize on-site testing on unprocessed biological samples. To achieve this, a microfluidic device will be integrated for sample handling and washing. In this study, we used killed virus preparation in pure solution. Further evaluation of the assay using real unprocessed biological sample is required to study the effect of sample matrix on sensitivity and specificity of this assay.

With Z-Lab, affordable, accurate, noninvasive testing for numerous diseases can become routine for every patient at an annual physical or even on a daily basis at home. Likewise, it will be inexpensive to test animals and areas of environmental concerns like watersheds on a regular basis. People with chronic conditions like cancer, HIV, or Lyme disease will be able to monitor themselves with Z-Lab at home and receive rapid treatment if a disease escalates. Z-Lab's ability to inexpensively test for multiple biomarkers at once, along with its ability to automatically send nonprivate information to databases, will enable scientists to identify thousands of new correlations and new lines of research.

ASSOCIATED CONTENT

Supporting Information

The Supporting Information is available free of charge on the ACS Publications website at DOI: 10.1021/acssensors.7b00432.

GMR sensing scheme, tablet app user interface, the sci-FLEXARRAYER S5 system, active and control sensor arrays, MACS particles, uniformity of magnetic field generated by coils (PDF)

AUTHOR INFORMATION

Corresponding Author

*E-mail: jpwang@umn.edu.

ORCID

Kai Wu: 0000-0002-9444-6112

DOI: 10.1021/acssensors.7b00432
ACS Sens. 2017, 2, 1594−1601

Author Contributions

[⊥]K.W., T.K., and V.D.K. contributed equally to this work.

Notes

The authors declare the following competing financial interest(s): J.-P.W. has equity and royalty interests in, and serves on the Board of Directors and the Scientific Advisory Board, for Zepto Life Technology LLC, a company involved in the commercialization of GMR Biosensing technology. The University of Minnesota also has equity and royalty interests in Zepto Life Tech LLC. These interests have been reviewed and managed by the University of Minnesota in accordance with its Conflict of Interest policies.

■ ACKNOWLEDGMENTS

We thank Maxim Cheeran for his helpful suggestions. We acknowledge XPRIZE Foundation and Nokia Sensing XCHALLENGE competition for motivating the design of the Z-Lab Diagnosis Platform which won Distinguished Prize Award. This work is supported by MNDrive: OVPR STEMMA program, Institute of Engineering in Medicine of the University of Minnesota, National Science Foundation MRSEC facility program, the Distinguished McKnight University Professorship, Centennial Chair Professorship, Robert F Hartmann Endowed Chair, and UROP program from the University of Minnesota. Parts of this work were carried out in the Characterization Facility, University of Minnesota, a member of the NSF-funded Materials Research Facilities Network (www.mrfn.org) via the MRSEC program.

■ REFERENCES

(1) Chen, Y.; Cui, D.; Zheng, S.; Yang, S.; Tong, J.; Yang, D.; Fan, J.; Zhang, J.; Lou, B.; Li, X.; Zhuge, X.; Ye, B.; Chen, B.; Mao, W.; Tan, Y.; Xu, G.; Chen, Z.; Chen, N.; Li, L. Simultaneous Detection of Influenza A, Influenza B, and Respiratory Syncytial Viruses and Subtyping of Influenza A H3N2 Virus and H1N1 (2009) Virus by Multiplex Real-Time PCR. *Journal of Clinical Microbiology* **2011**, *49* (4), 1653−1656.

(2) Lee, B. W.; Bey, R. F.; Baarsch, M. J.; Simonson, R. R. ELISA Method for Detection of Influenza A Infection in Swine. *J. Vet. Diagn. Invest.* **1993**, *5* (4), 510−515.

(3) Leuwerke, B.; Kitikoon, P.; Evans, R.; Thacker, E. Comparison of Three Serological Assays to Determine the Cross-Reactivity of Antibodies from Eight Genetically Diverse U.S. Swine Influenza Viruses. *J. Vet. Diagn. Invest.* **2008**, *20* (4), 426−432.

(4) Townsend, M. B.; Dawson, E. D.; Mehlmann, M.; Smagala, J. A.; Dankbar, D. M.; Moore, C. L.; Smith, C. B.; Cox, N. J.; Kuchta, R. D.; Rowlen, K. L. Experimental Evaluation of the FluChip Diagnostic Microarray for Influenza Virus Surveillance. *Journal of Clinical Microbiology* **2006**, *44* (8), 2863−2871.

(5) Amano, Y.; Cheng, Q. Detection of influenza virus: traditional approaches and development of biosensors. *Anal. Bioanal. Chem.* **2005**, *381* (1), 156−164.

(6) Ellis, J. S.; Zambon, M. C. Molecular diagnosis of influenza. *Rev. Med. Virol.* **2002**, *12* (6), 375−389.

(7) Miller, E.; Hoschler, K.; Hardelid, P.; Stanford, E.; Andrews, N.; Zambon, M. Incidence of 2009 pandemic influenza A H1N1 infection in England: a cross-sectional serological study. *Lancet* **2010**, *375* (9720), 1100−8.

(8) Payungporn, S.; Chutinimitkul, S.; Chaisingh, A.; Damrongwantanapokin, S.; Buranathai, C.; Amonsin, A.; Theamboonlers, A.; Poovorawan, Y. Single step multiplex real-time RT-PCR for H5N1 influenza A virus detection. *J. Virol. Methods* **2006**, *131* (2), 143−147.

(9) Driskell, J. D.; Jones, C. A.; Tompkins, S. M.; Tripp, R. A. One-step assay for detecting influenza virus using dynamic light scattering and gold nanoparticles. *Analyst* **2011**, *136* (15), 3083−3090.

(10) Lee, D.; Chander, Y.; Goyal, S. M.; Cui, T. Carbon nanotube electric immunoassay for the detection of swine influenza virus H1N1. *Biosens. Bioelectron.* **2011**, *26* (8), 3482−3487.

(11) Li, D.; Wang, J.; Wang, R.; Li, Y.; Abi-Ghanem, D.; Berghman, L.; Hargis, B.; Lu, H. A nanobeads amplified QCM immunosensor for the detection of avian influenza virus H5N1. *Biosens. Bioelectron.* **2011**, *26* (10), 4146−4154.

(12) Shen, F.; Wang, J.; Xu, Z.; Wu, Y.; Chen, Q.; Li, X.; Jie, X.; Li, L.; Yao, M.; Guo, X.; Zhu, T. Rapid Flu Diagnosis Using Silicon Nanowire Sensor. *Nano Lett.* **2012**, *12* (7), 3722−3730.

(13) Takeda, S.; Sbagyo, A.; Sakoda, Y.; Ishii, A.; Sawamura, M.; Sueoka, K.; Kida, H.; Mukasa, K.; Matsumoto, K. Application of carbon nanotubes for detecting anti-hemagglutinins based on antigen−antibody interaction. *Biosens. Bioelectron.* **2005**, *21* (1), 201−205.

(14) Tam, P. D.; Van Hieu, N.; Chien, N. D.; Le, A.-T.; Anh Tuan, M. DNA sensor development based on multi-wall carbon nanotubes for label-free influenza virus (type A) detection. *J. Immunol. Methods* **2009**, *350* (1−2), 118−124.

(15) Singh, R.; Sharma, A.; Hong, S.; Jang, J. Electrical immunosensor based on dielectrophoretically-deposited carbon nanotubes for detection of influenza virus H1N1. *Analyst* **2014**, *139* (21), 5415−5421.

(16) Horiguchi, Y.; Goda, T.; Matsumoto, A.; Takeuchi, H.; Yamaoka, S.; Miyahara, Y. Direct and label-free influenza virus detection based on multisite binding to sialic acid receptors. *Biosens. Bioelectron.* **2017**, *92*, 234−240.

(17) Patolsky, F.; Zheng, G.; Hayden, O.; Lakadamyali, M.; Zhuang, X.; Lieber, C. M. Electrical detection of single viruses. *Proc. Natl. Acad. Sci. U. S. A.* **2004**, *101* (39), 14017−14022.

(18) Shen, F.; Tan, M.; Wang, Z.; Yao, M.; Xu, Z.; Wu, Y.; Wang, J.; Guo, X.; Zhu, T. Integrating Silicon Nanowire Field Effect Transistor, Microfluidics and Air Sampling Techniques For Real-Time Monitoring Biological Aerosols. *Environ. Sci. Technol.* **2011**, *45* (17), 7473−7480.

(19) Lum, J.; Wang, R.; Hargis, B.; Tung, S.; Bottje, W.; Lu, H.; Li, Y. An Impedance Aptasensor with Microfluidic Chips for Specific Detection of H5N1 Avian Influenza Virus. *Sensors* **2015**, *15* (8), 18565−18578.

(20) Mak, A. C.; Osterfeld, S. J.; Yu, H.; Wang, S. X.; Davis, R. W.; Jejelowo, O. A.; Pourmand, N. Sensitive giant magnetoresistive-based immunoassay for multiplex mycotoxin detection. *Biosens. Bioelectron.* **2010**, *25* (7), 1635−1639.

(21) Kim, D.; Wang, S. X. A magneto-nanosensor immunoassay for sensitive detection of Aspergillus fumigatus allergen Asp f 1. *IEEE Trans. Magn.* **2012**, *48* (11), 3266−3268.

(22) Sun, X.; Lei, C.; Guo, L.; Zhou, Y. Separable detecting of Escherichia coli O157H: H7 by a giant magneto-resistance-based biosensing system. *Sens. Actuators, B* **2016**, *234*, 485−492.

(23) Shi, J.-J.; Lian, J.; Zhou, W.-W.; Shi, X.-Z.; Gao, Y.-H. Magnetoresistive Biosensor for Detection of Chloramphenicol Residue in Milk. *Fenxi Huaxue* **2012**, *40* (10), 1524−1529.

(24) Srinivasan, B.; Li, Y.; Jing, Y.; Xu, Y.; Yao, X.; Xing, C.; Wang, J. P. A Detection System Based on Giant Magnetoresistive Sensors and High-Moment Magnetic Nanoparticles Demonstrates Zeptomole Sensitivity: Potential for Personalized Medicine. *Angew. Chem., Int. Ed.* **2009**, *48* (15), 2764−2767.

(25) Krishna, V. D.; Wu, K.; Perez, A. M.; Wang, J.-P. Giant Magnetoresistance-based Biosensor for Detection of Influenza A Virus. *Front. Microbiol.* **2016**, DOI: 10.3389/fmicb.2016.00400.

(26) Wang, Y.; Wang, W.; Yu, L.; Tu, L.; Feng, Y.; Klein, T.; Wang, J.-P. Giant magnetoresistive-based biosensing probe station system for multiplex protein assays. *Biosens. Bioelectron.* **2015**, *70*, 61−68.

(27) Wang, W.; Wang, Y.; Tu, L.; Klein, T.; Feng, Y.; Wang, J.-P. Surface modification for Protein and DNA immobilization onto GMR biosensor. *IEEE Trans. Magn.* **2013**, *49* (1), 296−299.

(28) Wu, K.; Schliep, K.; Zhang, X.; Liu, J.; Ma, B.; Wang, J. P. Characterizing Physical Properties of Superparamagnetic Nanoparticles in Liquid Phase Using Brownian Relaxation. *Small* **2017**, *13* (22), 1604135.

DOI: 10.1021/acssensors.7b00432
ACS Sens. 2017, 2, 1594−1601

(29) Gaster, R. S.; Xu, L.; Han, S.-J.; Wilson, R. J.; Hall, D. A.; Osterfeld, S. J.; Yu, H.; Wang, S. X. Quantification of protein interactions and solution transport using high-density GMR sensor arrays. *Nat. Nanotechnol.* **2011**, *6* (5), 314−320.
(30) Wang, W.; Wang, Y.; Tu, L.; Feng, Y.; Klein, T.; Wang, J.-P. Magnetoresistive performance and comparison of supermagnetic nanoparticles on giant magnetoresistive sensor-based detection system. *Sci. Rep.* **2015**, *4*, 5716.
(31) Choi, J.; Gani, A. W.; Bechstein, D. J.; Lee, J.-R.; Utz, P. J.; Wang, S. X. Portable, one-step, and rapid GMR biosensor platform with smartphone interface. *Biosens. Bioelectron.* **2016**, *85*, 1−7.
(32) Klein, T.; Wang, Y.; Tu, L.; Yu, L.; Feng, Y.; Wang, W.; Wang, J.-P. Comparative analysis of several GMR strip sensor configurations for biological applications. *Sens. Actuators, A* **2014**, *216*, 349−354.
(33) Li, G.; Wang, S. X.; Sun, S. Model and experiment of detecting multiple magnetic nanoparticles as biomolecular labels by spin valve sensors. *IEEE Trans. Magn.* **2004**, *40* (4), 3000−3002.
(34) Li, Y.; Srinivasan, B.; Jing, Y.; Yao, X.; Hugger, M. A.; Wang, J.-P.; Xing, C. Nanomagnetic competition assay for low-abundance protein biomarker quantification in unprocessed human sera. *J. Am. Chem. Soc.* **2010**, *132* (12), 4388−4392.
(35) Srinivasan, B.; Li, Y.; Jing, Y.; Xu, Y.; Yao, X.; Xing, C.; Wang, J.-P. A Detection System Based on Giant Magnetoresistive Sensors and High-Moment Magnetic Nanoparticles Demonstrates Zeptomole Sensitivity: Potential for Personalized Medicine. *Angew. Chem., Int. Ed.* **2009**, *48* (15), 2764−2767.
(36) Lekcharoensuk, P.; Lager, K. M.; Vemulapalli, R.; Woodruff, M.; Vincent, A. L.; Richt, J. A. Novel Swine Influenza Virus Subtype H3N1, United States. *Emerging Infect. Dis.* **2006**, *12* (5), 787.

DOI: 10.1021/acssensors.7b00432
ACS Sens. 2017, 2, 1594−1601